



Quantum chemical study on the catalytic mechanism of Na/K on NO-char heterogeneous reactions during the coal reburning process*

Zheng-cheng WEN[†], Zhi-hua WANG^{†‡}, Jun-hu ZHOU, Ke-fa CEN

(State Key Laboratory of Clean Energy Utilization, Zhejiang University, Hangzhou 310027, China)

[†]E-mail: giani@zju.edu.cn; wangzh@zju.edu.cn

Received May 5, 2008; Revision accepted Sept. 9, 2008; Crosschecked Dec. 29, 2008

Abstract: Quantum chemical simulation was used to investigate the catalytic mechanism of Na/K on NO-char heterogeneous reactions during the coal reburning process. Both NO-char and NO-Na/K reactions were considered as three-step processes in this calculation. Based on geometry optimizations made using the UB3LYP/6-31G(d) method, the activation energies of NO-char and NO-Na/K reactions were calculated using the QCISD(T)/6-311G(d, p) method; Results showed that the activation energy of the NO-Na/K reaction (107.9/82.0 kJ/mol) was much lower than that of the NO-char reaction (245.1 kJ/mol). The reactions of NaO/KO and Na₂O/K₂O reduced by char were also studied, and their thermodynamics were calculated using the UB3LYP/6-31G(d) method; Results showed that both Na and K can be refreshed easily and rapidly by char at high temperature during the coal reburning process. Based on the calculations and analyses, the catalytic mechanism of Na/K on NO-char heterogeneous reactions during the coal reburning process was clarified.

Key words: Catalytic mechanism, Quantum chemistry, Sodium, Potassium, Char, NO

doi:10.1631/jzus.A0820345

Document code: A

CLC number: TK474

INTRODUCTION

Recently, the emission of nitrogen oxides from coal combustion has had a serious impact on the environment. Great effort has been made to reduce NO_x economically and effectively. Nowadays, reburning is considered to be one of the most promising NO_x control technologies because of its high efficiency and low cost, especially for retrofit applications, as demonstrated in laboratory reactors and in full-scale boilers (Smoot *et al.*, 1998; Hampartsoumian *et al.*, 2003). Gaseous hydrocarbon fuels such as natural gas are usually chosen for reburning due to their high NO_x reduction efficiency and lower retrofit cost. Because of the limited supplies of gaseous fuels in China,

many researchers are trying to use coal as a substitute (Moyeda *et al.*, 1995; Zhou *et al.*, 2004). Compared with gaseous fuels, pulverized coal is a more economical reburning fuel and is suitable for use in most coal-fired utility boilers. However, only 50%~70% NO_x reduction efficiency is achieved using the original coal reburning technology. Thus, many attempts have been made to improve the NO_x reduction efficiency of coal reburning technology.

The mechanism of coal reburning was considered to be very complicated because of the heterogeneous character of coal combustion and the effects of coal rank, ash composition, and fuel-bound nitrogen content. Apart from the homogeneous reactions between hydrocarbon radicals and NO, the heterogeneous NO-char reaction is also important during the coal reburning process (Chen and Ma, 1997; Liu *et al.*, 1997; Maly *et al.*, 1999). The mineral matter, which is usually coherent in the coal ash, has been shown to have an active catalytic effect on the

[†] Corresponding author.

* Project supported by the National Science Fund for Distinguished Young Scholars (No. 50525620), and the Key Project of Chinese National Programs for Fundamental Research and Development (No. 2006CB200303), China

heterogeneous reaction between NO and char. Zhao *et al.* (2002a; 2002b; 2003) investigated the catalytic effect of sodium, calcium and iron impregnated on coal chars on the NO-char reaction under various atmospheres in a quartz fixed bed reactor. Zhong *et al.* (2003) and Zhong and Tang (2007) investigated the kinetic parameters of the NO-char reaction by adding KOH/NaOH as a catalyst at high temperature. Illán-Gómez *et al.* (1999; 2000; 2001) and García-García *et al.* (1997; 2002) studied the catalytic reduction of NO by carbon supporting potassium, calcium and various transition metals (Fe, Co, Ni, Cu). Wang *et al.* (2007) studied the catalytic effect of mineral matter (Na, K, Ca, and Fe) on NO reduction efficiency during the coal reburning process in an entrained flow reactor. However, most studies focused on the macroscopic catalytic effect and little attention has been paid to the microscopic catalytic mechanism. Despite its fundamental importance, the catalytic mechanism of mineral matter on NO-char heterogeneous reactions is still unclear. To further improve the NO_x reduction efficiency during the coal reburning process, the microscopic catalytic mechanism of mineral matter on NO-char heterogeneous reactions was investigated using quantum chemistry theory. Sodium and potassium, which usually have better performance in heterogeneous NO-char reactions during the coal reburning process, were selected as the typical mineral matter. The microscopic mechanisms of NO-char and NO-Na/K reactions were analyzed using quantum chemical calculations and the results were discussed. Moreover, the activation energies of the reactions were calculated and compared in the same level of calculation. Finally, the catalytic mechanism of Na/K on NO-char heterogeneous reactions during the coal reburning process were discussed and clarified.

CALCULATION DETAILS

Owing to the limits of quantum chemical calculation ability, the porosity, specific area and structure of the traditional char cannot be considered. Only atomic C was used as a model of char in the current calculation. The boiling points of Na (882.9 °C) and especially K (774 °C) are not very high, and most Na/K exists as metallic vapor at high temperature in reburning or combustion (Takuwa and Naruse, 2007).

So, atomic Na and K were also used as models of sodium and potassium in the char surface to compare with the calculated results of the NO-char reaction.

The Gaussian 2003 package (Frisch *et al.*, 2003) was used for the quantum chemical calculations. All the geometry optimizations of stationary points along the reactions were made using the quantum chemistry UB3LYP method at the 6-31G(d) basis function level (Lee *et al.*, 1988; Becke, 1993). The optimized stationary points were characterized as intermediates or transition states by diagonalizing the Hessian matrix and analyzing the vibrational normal modes. In this way, the stationary points can be classified as intermediates if no imaginary frequencies are shown or as transition states if only one imaginary frequency is obtained. Furthermore, the particular nature of the transition states was determined by calculation of the intrinsic reaction coordinate (IRC) (Gonzalez and Schlegel, 1989) and the vibrational analysis of imaginary frequency.

Based on geometry optimizations made using the UB3LYP/6-31G(d) method, the potential energies of stationary points of most reactions were calculated using the QCISD(T)/6-311G(d, p) method (Gauss and Cremer, 1988; Salter *et al.*, 1989). After correction using zero-point energies (ZPE), the activation energies (ΔE) of most sub-reactions were calculated. Also, the enthalpy (ΔH) and the Gibbs free energy (ΔG) of some reactions at high temperature were calculated at the UB3LYP/6-31G(d) level of theory, according to the following equations (Foresman and Frisch, 1996):

$$\Delta H(T) = \Delta E_e^0 + \Delta H_{\text{cor}}(T),$$

$$\Delta G(T) = \Delta E_e^0 + \Delta G_{\text{cor}}(T),$$

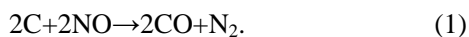
where T is the temperature, ΔE_e^0 is the energy difference between products and reactants at 0 K, ΔH_{cor} and ΔG_{cor} are the difference of thermal energy correction to enthalpy and Gibbs free energy between products and reactants, respectively.

The ZPE, ΔH_{cor} and ΔG_{cor} were calculated at the UB3LYP/6-31G(d) level of theory, as used for the geometry optimizations. To obtain more reliable values, the raw calculated values of ZPE, ΔH_{cor} and ΔG_{cor} were scaled by 0.9613 to account for their average overestimation when the UB3LYP/6-31G(d) method is used (Scott and Random, 1996).

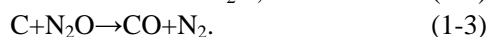
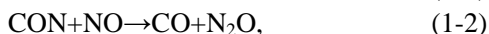
RESULTS AND DISCUSSION

NO-char reaction

Although the heterogeneous reaction between NO and coal char has been widely studied (Suzuki *et al.*, 1994; Chambrion *et al.*, 1996; Aarna and Suuberg, 1997; Chen and Yang, 1998; Kyotani and Tomita, 1999; Yang *et al.*, 2000; Arenillas and Josea, 2002; Andersson *et al.*, 2003), there is still some debate about the microscopic reaction mechanism of NO-char heterogeneous reactions. For simplicity, our work was focused on the following reaction:



For removing atomic N and eventually forming N_2 , Reaction Eq.(1) was considered to be the most important reaction in the system of the NO-char heterogeneous reaction. Based on the conclusion of earlier studies, Reaction Eq.(1) is considered here to be a three-step reaction. The chemical equations of the three sub-reactions are:



The proposed mechanism of Reaction Eq.(1) was confirmed by some earlier work. In the theoretical work of Andersson *et al.*(2003), linear CON was considered to be one of the earlier products of the reaction between atomic C and NO. The experimental research of Arenillas and Josea (2002) showed that N_2O was formed as an important intermediate in the system of the C-NO reaction. Considering the valence change of atomic N (+2→+1→0), it can be concluded that N_2 was likely to be formed through the intermediate N_2O . Therefore, Reaction Eq.(1-2) was reasonable. Moreover, the experimental research of Noda *et al.*(1999) showed that N_2O reacts with carbon edge sites directly, there is little surface nitrogen species accumulated on carbon and there is little $\text{N}\equiv\text{N}$ splitting in the reaction. This is in good agreement with Reaction Eq.(1-3). To confirm rationality and reliability, the proposed mechanism of Reaction Eq.(1) was investigated in detail using quantum chemical calculation. The reaction processes and kinetic mechanisms of Reactions Eq.(1-1) and Eq.(1-3) and the

thermochemistry of Reaction Eq.(1-2) were also studied and are discussed below.

The geometry optimizations of stationary points along Reaction Eq.(1-1) and Eq.(1-3) were made using the UB3LYP/6-31G(d) method. The microscopic reaction processes based on analyses of the stationary points are shown in Figs.1a and 1c. Because neither stable intermediate nor transition states were found during Reaction Eq.(1-2) in the UB3LYP/6-31G(d) calculation, Reaction Eq.(1-2) could be a direct reaction and its kinetic mechanism could not be studied in detail. So we turned to the thermochemistry of Reaction Eq.(1-2). The geometries of the reactant and product of Reaction Eq.(1-2) were optimized using the UB3LYP/6-31G(d) method. The results are shown in Fig.1b.

There are two possible reaction paths in Reaction Eq.(1-1) (Fig.1a). Path (1) and path (2) are separated from the triangular CNO (M_1), which is formed first as an intermediate. Linear CNO (M_2) is formed through the transition state (TS_1) in path (1), while linear CON (M_3) is formed through the transition state (TS_2) in path (2). During path (1), the distance between atomic C and N reduces gradually ($\infty \text{ nm}\rightarrow 0.1341 \text{ nm}\rightarrow 0.1247 \text{ nm}\rightarrow 0.1214 \text{ nm}$, where ∞ denotes the distance exceeding the range of bond forming) and the bond angle $\angle\text{CNO}$ increases gradually ($60.9^\circ\rightarrow 100.9^\circ\rightarrow 180.0^\circ$). The changes in bond distance and bond angle indicate the forming of C–N bonds and linear CNO. During path (2), the distance between atomic C and O reduces gradually ($\infty \text{ nm}\rightarrow 0.1405 \text{ nm}\rightarrow 0.1308 \text{ nm}\rightarrow 0.1185 \text{ nm}$) and the bond angle $\angle\text{CON}$ increases gradually ($56.5^\circ\rightarrow 124.4^\circ\rightarrow 180.0^\circ$). The changes in bond distance and bond angle indicate the forming of C–O bonds and linear CON.

Reaction Eq.(1-3) is a one-step reaction and no intermediate is formed (Fig.1c). There is only one transition state (TS) formed in the reaction and it is in one plane. The products are immediately formed through the TS. During the reaction process, the distance between atomic C and O reduces gradually ($\infty \text{ nm}\rightarrow 0.1370 \text{ nm}\rightarrow 0.1138 \text{ nm}$) and the distance between atomic O and the adjacent atomic N increases gradually ($0.1192 \text{ nm}\rightarrow 0.1352 \text{ nm}\rightarrow \infty \text{ nm}$). The changes in bond distance indicate the forming of C–O bonds and the breaking of N–O bonds.

Vibration frequency analyses were used to verify

intermediates and transition states. The results are shown in Table 1. All the vibration frequencies of intermediates were positive numbers, and there was only one imaginary vibration frequency of each transition state. This shows that the intermediates are the stable points of potential surface and the transition states really exist. IRC calculations and vibrational analysis of imaginary frequencies were also carried out. For Reaction Eq.(1-1), TS_1 connects the intermediate M_1 and the product M_2 , while TS_2 connects the intermediate M_1 and the product M_3 . For Reaction Eq.(1-3), TS connects the reactant and the product. This shows that the microscopic reaction processes were reasonable.

Based on geometry optimizations made using the UB3LYP/6-31G(d) method, all potential energies of stationary points along Reactions Eq.(1-1) and Eq.(1-3) were calculated using the QCISD(T)/6-311G(d, p) method. Fig.2 shows the variation in energies in the reaction processes of Reactions Eqs.(1-1) and (1-3) after correction with ZPE. The activation energies of Reactions Eq.(1-1) and Eq.(1-3)

were calculated according to transition state theory (TST). Because the linear CNO does not have the potential to remove atomic N and eventually form N_2 , only the activation energy of path (2) (about 245.1 kJ/mol) was calculated for Reaction Eq.(1-1). For Reaction Eq.(1-3), the calculated activation energy was lower (about 125.5 kJ/mol).

Based on geometry optimizations made using the UB3LYP/6-31G(d) method, the enthalpy (ΔH) and the Gibbs free energy (ΔG) of Reaction Eq.(1-2) at high temperature (873~1673 K) were calculated. The results (Fig.2) show that ΔH is not sensitive to temperatures from 873 to 1673 K, and its steady value is about -700 kJ/mol. The negative value of ΔH shows that Reaction Eq.(1-2) is exothermic. Although the value of ΔG at temperatures from 873~1673 K is negative, too, varying from -670 to -650 kJ/mol, the absolute value of ΔG decreases linearly with increasing temperature,. According to the theory of thermodynamics, a large negative ΔG means that the reaction has a tendency to proceed spontaneously and its activation energy can be considered to be very low.

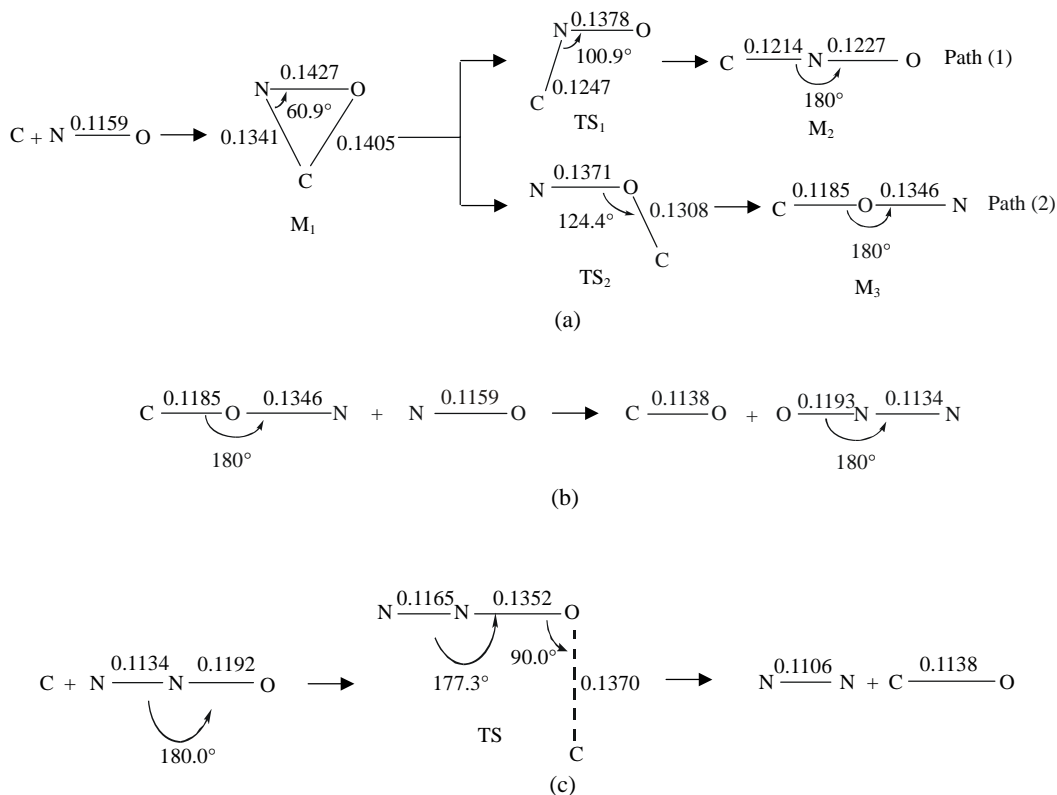
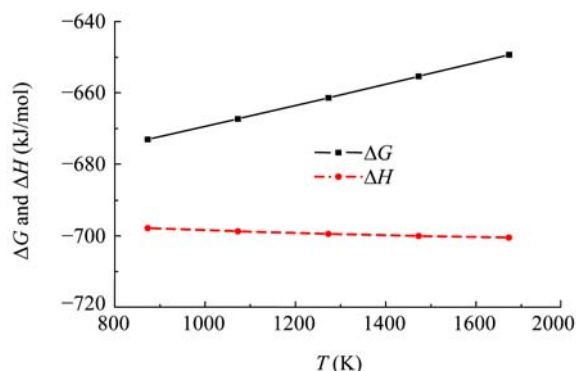


Fig.1 Optimized geometries of the stationary points (a) along the $C+NO \rightarrow CON$ reaction paths; (b) in the $CON+NO \rightarrow CO+N_2O$ reaction; (c) along the $C+N_2O \rightarrow CO+N_2$ reaction paths. Bond distances are given in nm

Table 1 Vibrational frequency (cm^{-1}) of transition states (TS) and intermediates (M)

Reaction	Frequency (cm^{-1})				
1-1	M ₁	565.71	958.89	1477.04	
	TS ₁	-585.12	1014.31	1660.17	
	M ₂	293.20	406.36	675.96	1694.74
	TS ₂	-614.25	786.95	1098.62	
1-3	M ₃	308.40	409.93	1207.70	1953.63
	TS	-1474.68	331.82	397.08	743.13
2-1	M ₁	224.47	419.50	1472.48	
	TS ₁	-122.13	375.47	1568.90	
	M ₂	182.58	279.08	396.67	1663.39
	TS ₂	-102.04	285.63	1543.46	
2-2	M ₃	128.96	241.19	396.10	1428.19
	M	31.85	38.71	276.55	373.26
	M	420.39	739.85	1170.73	1260.47
	TS	1510.13	-659.64	33.09	56.33
2-3	M	164.24	198.12	398.75	575.81
	M	769.31	1739.00		
	TS	-498.37	143.31	157.77	398.24
	TS	529.35	1990.73		
3-1	M ₁	251.87	336.85	1432.47	
	TS ₁	-103.31	314.98	1478.47	
	M ₂	147.78	229.99	294.62	1592.94
	TS ₂	-169.37	261.99	1554.41	
3-2	M ₃	109.80	157.99	269.76	1447.48
	M	72.10	102.83	276.65	301.47
	M	386.43	666.37	939.95	1086.96
	TS	1171.33	-515.79	52.37	100.43
3-3	M	138.93	162.36	318.72	571.60
	M	857.31	1718.01		
	TS	-488.39	116.22	127.93	332.35
	TS	475.32	2032.61		

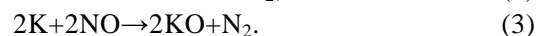
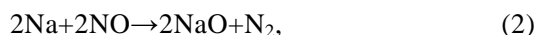
From the calculation and analysis of Reactions Eqs.(1-1), (1-2) and (1-3), the whole activation energy of Reaction Eq.(1) could be obtained. Although the kinetic mechanism of Reaction Eq.(1-2) cannot be investigated using the UB3LYP/6-31G(d) method, the results of thermochemistry calculations indicated that Reaction Eq.(1-2) is a spontaneous reaction and its activation energy can be considered to

**Fig.2** ΔG and ΔH of the reaction $\text{CON}+\text{NO}\rightarrow\text{CO}+\text{N}_2\text{O}$

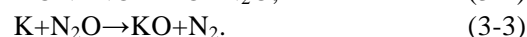
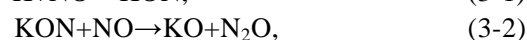
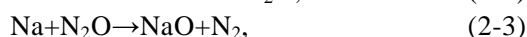
be very low, much lower than that of Reactions Eq.(1-1) and Eq.(1-3). So, after comparing the activation energies of the three reactions, it can be concluded that Reaction Eq.(1-1) is the rate-determining reaction. The whole activation energy of Reaction Eq.(1) was estimated to be 245.1 kJ/mol. This is close to experimental results, which are usually in the range of 180~220 kJ/mol (Aarna and Suuberg, 1997). Given that only atomic C was used as the model of char in the calculations, the rough agreement between the calculated results and the experimental results was acceptable.

NO-Na/K reaction

To compare with the NO-char reaction, only atomic Na/K was used as the model of sodium/potassium in the char surface. For simplicity, the calculation was focused on the following reactions:



As with the proposal mechanism of Reaction Eq.(1), Reactions Eqs.(2) and (3) were also considered to be three-step reactions. The chemical equations of their sub-reactions were:



The proposed mechanisms of Reactions Eqs.(2)

and (3) were investigated in detail using quantum chemical calculations. The kinetic mechanisms of all six sub-reactions were calculated and analyzed as follows. The geometry optimizations of stationary points along all six sub-reactions involved were made using the UB3LYP/6-31G(d) method. The microscopic reaction processes based on the analysis of each stationary point, are shown in Fig.3.

The reaction processes of Reactions Eqs.(2-1) and (3-1) are very similar (Figs.3a and 3b). Moreover, they are similar to that of Reaction Eq.(1-1). As the reaction process of Reaction Eq.(1-1) was analyzed in details above, the reaction processes of Reactions Eqs.(2-1) and (3-1) are not explored further in this paper. The changes in geometric configurations about intermediates and transition states (Figs.3a and 3b), describe the reaction processes clearly.

All the reaction processes of Reactions Eqs.(2-2), (2-3), (3-2) and (3-3) are very similar (Figs.3c~3f). In each reaction, a stable intermediate M is first formed which then breaks down into products via the transition state.

The changes in geometric configurations about intermediates and transition states during the processes of reactions are summarized in Table 2. The changes describe the reaction processes clearly.

Vibration frequency analyses and IRC calculations were carried out to confirm the reaction processes of all the six sub-reactions. The results of vibration frequency analyses are shown in Table 1. Intermediates do not have any imaginary vibration frequency, while each transition state has only one imaginary vibration frequency. This shows that intermediates are the stable points of potential surface and that transition states really exist. Moreover, the results of IRC calculations showed that all the transition states connected reactants to intermediates or intermediates to products. This showed that the proposed reaction processes were reasonable.

Based on geometry optimizations made using the UB3LYP/6-31G(d) method, all potential energies of stationary points along the six sub-reactions were calculated using the QCISD(T)/6-311G(d, p) method. Fig.4 shows the energy variation in reaction processes of all the six reactions after correction with ZPE. The activation energies of all the six sub-reactions were calculated according to the TST. The calculated activation energies of Reactions Eqs.(2-1), (2-2), (2-3),

(3-1), (3-2) and (3-3) were 82.0, 107.9, 4.6, 82.0, 75.3 and 5.9 kJ/mol, respectively.

By comparing activation energies of Reactions Eqs.(2-1), (2-2) and (2-3), it can be concluded that Reaction Eq.(2-2) was the rate-determining reaction and the whole activation energy of Reaction Eq.(2) was 107.9 kJ/mol. However, by comparing activation energies of reactions Eqs.(3-1), (3-2) and (3-3), it can be concluded that Reaction Eq.(3-1) was the rate-determining reaction and the whole activation energy of Reaction Eq.(3) was 82.0 kJ/mol.

Discussion of catalytic mechanism

Based on the analyses and calculations above, activation energies of Reactions Eqs.(1), (2) and (3) were compared (Fig.5). The results show that the activation energies of both Reactions Eqs.(2) and (3) are much lower than that of Reaction Eq.(1). Thus, the reduction of NO by sodium or potassium is more efficient and more rapid than that by char.

The reactions of NaO/KO and Na₂O/K₂O reduced by char are also important in the catalytic system in relation to the refresh of sodium and potassium. Because no stationary point was found using the UB3LYP/6-31G(d) method, only the thermodynamics of these reactions were studied. Based on geometry optimizations made using the UB3LYP/6-31G(d) method, the enthalpy (ΔH) and the Gibbs free energies (ΔG) of these reactions at high temperatures (873~1673 K) were calculated. The absolute values of both ΔH and ΔG at high temperatures are quite large, in the range of 850~1050 kJ/mol (Figs.6a and 6b). It can be concluded that these reactions are spontaneous reactions, and their activation energies can be considered to be very low. Thus, both sodium and potassium could be refreshed easily and rapidly by char at high temperatures during the coal reburning process.

From the calculations and analyses above, the catalytic mechanism of Na/K on NO-char heterogeneous reactions during the coal reburning process was determined (Fig.7). As shown, the chemical equations were also used to depict the catalytic mechanism. During the coal reburning process, Na/K reacts with NO to form N₂ and NaO/KO, and then NaO/KO is easily reduced to Na/K by char at high temperatures. Considering that the activation energy of the NO-sodium/potassium reaction is much lower than

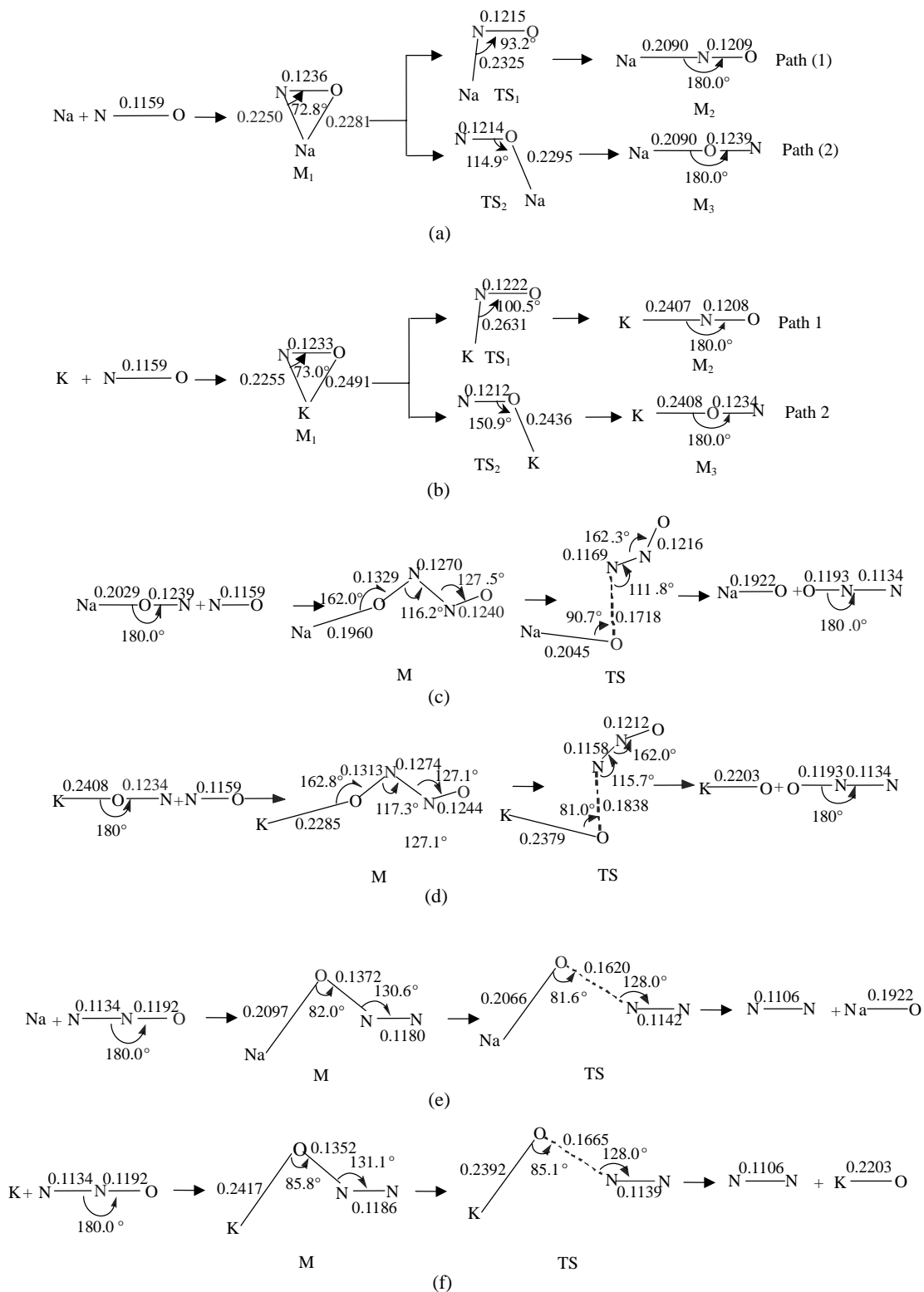
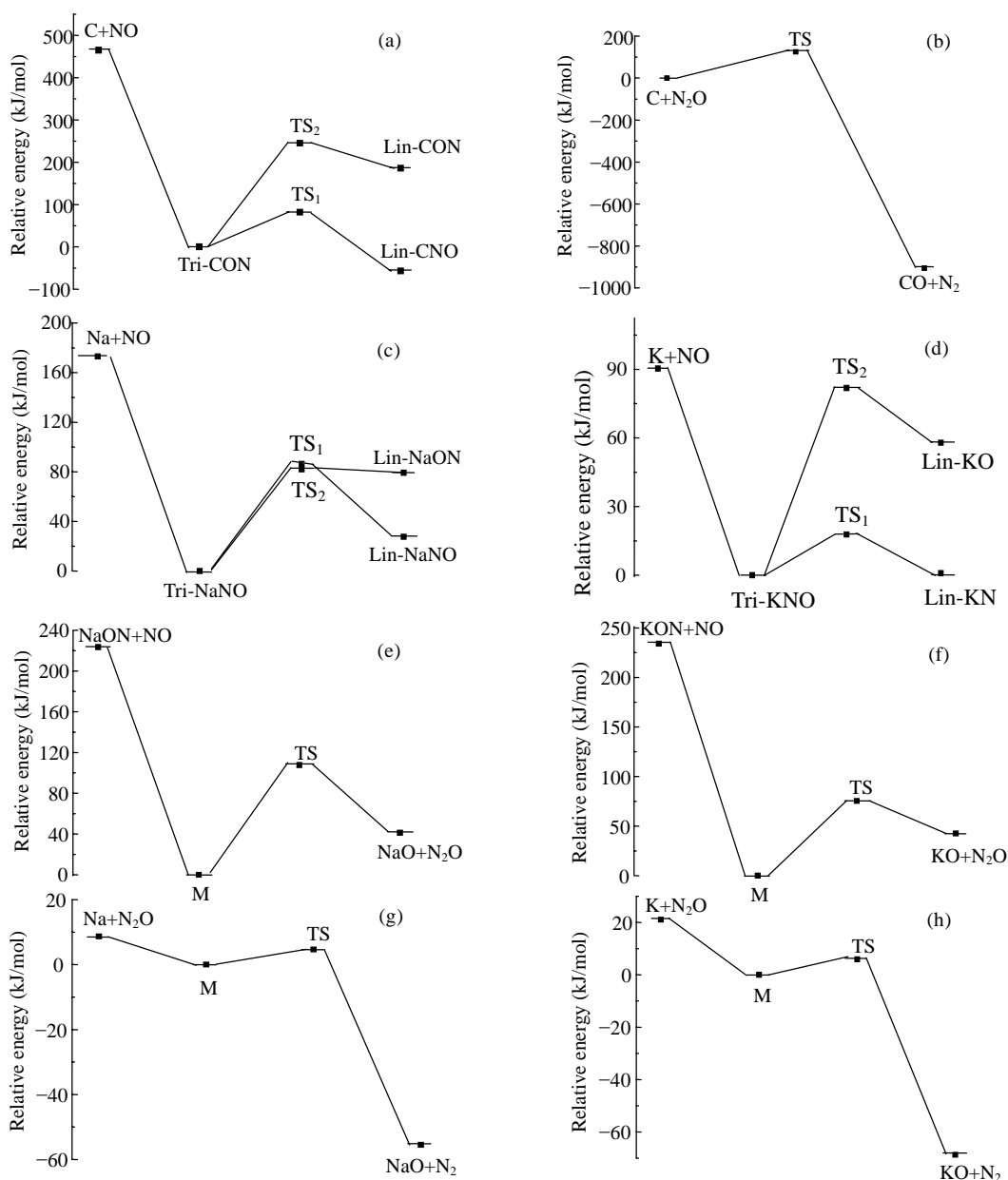


Fig.3 Optimized geometries of the stationary points along the (a) $\text{Na} + \text{NO} \rightarrow \text{NaON}$ reaction paths; (b) $\text{K} + \text{NO} \rightarrow \text{KON}$ reaction paths; (c) $\text{NaON} + \text{NO} \rightarrow \text{NaO} + \text{N}_2\text{O}$ reaction paths; (d) $\text{KON} + \text{NO} \rightarrow \text{KO} + \text{N}_2\text{O}$ reaction paths; (e) $\text{NaON} + \text{NO} \rightarrow \text{NaO} + \text{N}_2\text{O}$ reaction paths; (f) $\text{KON} + \text{NO} \rightarrow \text{KO} + \text{N}_2\text{O}$ reaction paths. Bond distances are given in nm

Table 2 Changes in geometric configurations along the reaction processes (∞ denotes the distance exceeding the range of bond forming)

Reaction	Changes of bond distance (nm)		Description	Indication
Eq.(2-2)	N-N	$\infty \rightarrow 0.1270 \rightarrow 0.1169 \rightarrow 0.1134$	Decrease gradually	Forming of N-N bond
	O-N	$0.1239 \rightarrow 0.1319 \rightarrow 0.1718 \rightarrow \infty$	Increase gradually	Breaking of O-N bond
Eq.(3-2)	N-N	$\infty \rightarrow 0.1274 \rightarrow 0.1158 \rightarrow 0.1134$	Decrease gradually	Forming of N-N bond
	O-N	$0.1234 \rightarrow 0.1313 \rightarrow 0.1838 \rightarrow \infty$	Increase gradually	Breaking of O-N bond
Eq.(3-2)	Na-O	$\infty \rightarrow 0.2097 \rightarrow 0.2066 \rightarrow 0.1922$	Decrease gradually	Forming of Na-O bond
	O-N	$0.1192 \rightarrow 0.1372 \rightarrow 0.1620 \rightarrow \infty$	Increase gradually	Breaking of O-N bond
Eq.(3-3)	K-O	$\infty \rightarrow 0.2417 \rightarrow 0.2392 \rightarrow 0.2203$	Decrease gradually	Forming of K-O bond
	O-N	$0.1192 \rightarrow 0.1352 \rightarrow 0.1665 \rightarrow \infty$	Increase gradually	Breaking of O-N bond

**Fig.4** Potential energies of stationary points along different reaction paths. (a) $C+NO \rightarrow CON$; (b) $C+N_2O \rightarrow CO+N_2$; (c) $Na+NO \rightarrow NaON$; (d) $K+NO \rightarrow KON$; (e) $NaON+NO \rightarrow NaO+N_2O$; (f) $KON+NO \rightarrow KO+N_2O$; (g) $Na+N_2O \rightarrow NaO+N_2$; (h) $K+N_2O \rightarrow KO+N_2$

that of NO-char reaction, it can be clearly concluded that sodium/potassium is an effective catalyst for the NO-char heterogeneous reaction.

CONCLUSION

In this paper, the catalytic mechanism of Na/K on the NO-char heterogeneous reaction during the coal reburning process was investigated in detail using quantum chemical calculation. Both NO-char and NO-Na/K reactions were considered as three-step processes in this calculation. Based on geometry

optimizations made using the UB3LYP/6-31G(d) method, the activation energies of NO-char and NO-Na/K reactions were calculated using the QCISD(T)/6-311G(d, p) method. Results showed that the activation energy of the NO-Na/K (107.9/82.0 kJ/mol) reaction was much lower than that of the NO-char reaction (245.1kJ/mol). Moreover, the reactions of NaO/KO and Na₂O/K₂O reduced by char were also studied, and their thermodynamics were calculated using the UB3LYP/6-31G(d) method. Results showed that both the absolute values of ΔH and ΔG at high temperatures were quite big, in the range of 850~1050 kJ/mol. Thus, it can be concluded that both Na and K can be refreshed easily and rapidly by char at high temperatures during the coal reburning process.

According to the calculations and analyses above, the catalytic mechanism of Na/K on the NO-char heterogeneous reaction during the coal reburning process can be clarified. Thus, it was confirmed in theory that the mineral matter was an effective catalyst for the NO-char heterogeneous reaction. The results supported the theory that adding mineral matter to reburning coal would be an efficient method to improve NO_x reduction efficiency in the coal reburning process. This is the first time that

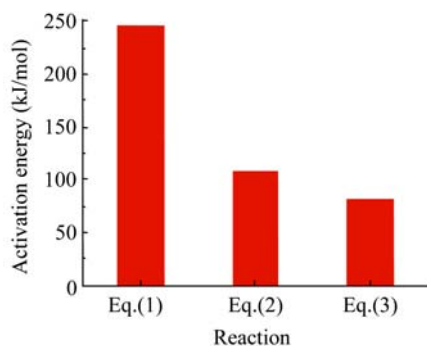


Fig.5 Activation energies of reactions
 Eq.(1): 2C+2NO→2CO+N₂; Eq.(2): 2Na+2NO→2NaO+N₂;
 Eq.(3): 2K+2NO→2KO+N₂

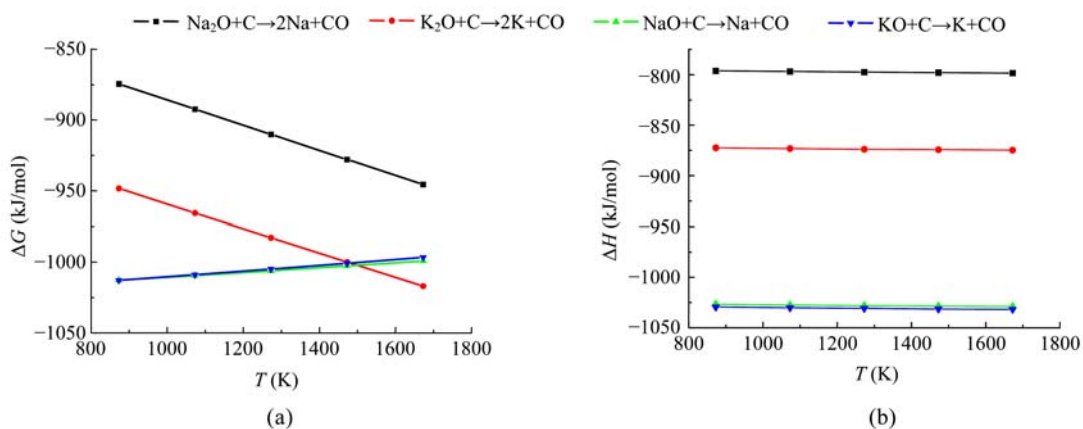


Fig.6 ΔG (a) and ΔH (b) of reactions at high temperature

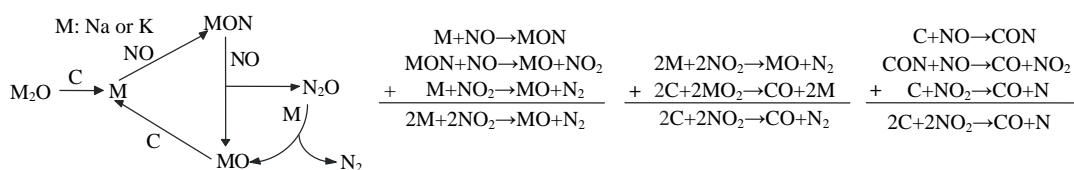


Fig.7 Catalytic mechanism of Na/K on NO-char heterogeneous reactions during the coal reburning process

quantum chemical theory has been used for investigating the catalytic mechanism of mineral matter on the NO-char heterogeneous reaction during the coal reburning process. So, only a simple model is used in the present work. In future work, more accurate models such as aromatic structures will be used as the model of char and more accurate activation energies of reactions will be obtained.

References

- Aarna, I., Suuberg, E.M., 1997. A review of the kinetics of the nitric oxide-carbon reaction. *Fuel*, **76**(6):475-491. [doi:10.1016/S0016-2361(96)00212-8]
- Andersson, S., Marković, N., Nyman, G., 2003. Computational studies of the kinetics of the C+NO and O+CN reactions. *The Journal of Physical Chemistry A*, **107**(28):5439-5447. [doi:10.1021/jp0222604]
- Arenillas, A., Josea, J.P., 2002. Nitric oxide reduction in coal combustion: role of char surface complexes in heterogeneous reactions. *Environmental Science & Technology*, **36**(24):5498-5503. [doi:10.1021/es0208198]
- Becke, A.D., 1993. Density functional thermochemistry III. The role of exact exchange correlation functions. *The Journal of Chemical Physics*, **98**(7):5648-5652. [doi:10.1063/1.464913]
- Chambrion, P., Suzuki, T., Zhang, Z.G., 1996. XPS of nitrogen-containing functional groups formed during the C-NO reaction. *Energy and Fuels*, **11**(3):681-685. [doi:10.1021/ef960109I]
- Chen, N., Yang, R.T., 1998. Ab initio molecular orbital study of the unified mechanism and pathways for gas-carbon reactions. *The Journal of Physical Chemistry A*, **102**(31):6348-6356. [doi:10.1021/jp981518g]
- Chen, W.Y., Ma, L., 1997. Effect of heterogeneous mechanisms during reburning of nitrogen oxide. *AIChE Journal*, **42**(7):1968-1976. [doi:10.1002/aic.690420717]
- Foresman, J.B., Frisch, A., 1996. *Exploring Chemistry with Electronic Structure Methods* (2nd Ed.). Gaussian, Pittsburgh, PA.
- Frisch, M.J., Trucks, G.W., Pople, J.A., Schlegel, H.B., Scuseria, G.E., Robb, M.A., Cheeseman, J.R., Montgomery, J.A., Vreven, J.T., Kudin, K.N., et al., 2003. Gaussian 03. Gaussian, Inc., Pittsburgh, PA.
- García-García, A., Illán-Gómez, M.J., Linares-Solano, A., Salinas-Martínez de Lecea, C., 1997. Potassium-containing briquetted coal for the reduction of NO. *Fuel*, **76**(6):499-505. [doi:10.1016/S0016-2361(97)00009-4]
- García-García, A., Illán-Gómez, M.J., Linares-Solano, A., Salinas-Martínez de Lecea, C., 2002. NO_x reduction by potassium-containing coal briquettes: Effect of preparation procedure and potassium content. *Energy and Fuels*, **16**(3):569-574. [doi:10.1021/ef0101208]
- Gauss, J., Cremer, C., 1988. Analytical evaluation of energy gradients in quadratic configuration interaction theory. *Chemical Physics Letters*, **150**(3-4):280-286. [doi:10.1016/0009-2614(88)80042-3]
- Gonzalez, C., Schlegel, H.B., 1989. An improved algorithm for reaction path following. *The Journal of Chemical Physics*, **90**(4):2154-2159.
- Hampartsoumian, E., Folayan, O.O., Nimmo, W., 2003. Optimisation of NO_x reduction in advanced coal reburning systems and the effect of coal type. *Fuel*, **82**(4):373-384. [doi:10.1016/S0016-2361(02)00311-3]
- Illán-Gómez, M.J., Raymundo-Piñero, E., García-García, A., Linares-Solano, A., Salinas-Martínez de Lecea, C., 1999. Catalytic NO_x reduction by carbon supporting metals. *Applied Catalysis B: Environmental*, **20**(4):267-275. [doi:10.1016/S0926-3373(98)00119-2]
- Illán-Gómez, M.J., Brandán, S., Linares-Solano, A., Salinas-Martínez de Lecea, C., 2000. NO_x reduction by carbon supporting potassium-bimetallic catalysts. *Applied Catalysis B: Environmental*, **25**(1):11-18. [doi:10.1016/S0926-3373(99)00120-4]
- Illán-Gómez, M.J., Brandán, S., Salinas-Martínez de Lecea, C., Linares-Solano, A., 2001. Improvements in NO_x reduction by carbon using bimetallic catalysts. *Fuel*, **80**(14):2001-2005. [doi:10.1016/S0016-2361(01)00091-6]
- Kyotani, T., Tomita, A., 1999. Analysis of the reaction of carbon with NO/N₂O using Ab initio molecular orbital theory. *The Journal of Physical Chemistry B*, **103**(17):3434-3441. [doi:10.1021/jp9845928]
- Lee, C., Yang, W., Parr, R.G., 1988. Development of the Colle-Salvetti correlation-energy formula into a functional of the electron density. *Physical Review B*, **37**(2):785-789. [doi:10.1103/PhysRevB.37.785]
- Liu, H., Hampartsoumian, E., Gibbs, B.M., 1997. Evaluation of the optimal fuel characteristics for efficient NO reduction by coal reburning. *Fuel*, **76**(11):985-993. [doi:10.1016/S0016-2361(97)00114-2]
- Maly, P.M., Zamansky, V.M., Locho, R.P., 1999. Alternative fuel reburning. *Fuel*, **78**(3):327-334. [doi:10.1016/S0016-2361(98)00161-6]
- Moyeda, D.K., Li, B., Maly, P., 1995. Experimental/Modeling Studies of the Use of Coal-based Reburning Fuels for NO_x Control. 12th International Pittsburgh Coal Conference, the Combustion Institute, Pittsburgh, USA, p.1119-1124.
- Noda, K., Chambrion, P., Kyotani, T., Tomita, A., 1999. A study of the N₂ formation mechanism in carbon-N₂O reaction by using isotope gases. *Energy and Fuels*, **13**(4):941-946. [doi:10.1021/ef9900132]
- Salter, E.A., Trucks, G.W., Bartlett, R.J., 1989. Analytic energy derivatives in many-body methods: First derivatives. *The Journal of Chemical Physics*, **90**(3):1752-1766. [doi:10.1063/1.456069]
- Scott, A.P., Random, L., 1996. Harmonic vibrational frequencies: an evaluation of Hartree-Fock, Moller-Plesset, quadratic configuration interaction, density functional theory, and semiempirical scale factors. *The Journal of Physical Chemistry*, **100**(41):16502-16513. [doi:10.1021/jp960976r]
- Smoot, L.D., Hill, S.C., Xu, H., 1998. NO_x control through

- reburning. *Progress in Energy and Combustion on Science*, **24**(5):385-408. [doi:10.1016/S0360-1285(97)00022-1]
- Suzuki, T., Kyotani, T., Tomita, A., 1994. Study on the carbon-nitric oxide reaction in the presence of oxygen. *Industrial & Engineering Chemistry Research*, **33**(11):2840-2845. [doi:10.1021/ie00035a038]
- Takuwa, T., Naruse, I., 2007. Detailed kinetic and control of alkali metal compounds during coal combustion. *Fuel Processing Technology*, **88**(11-12):1029-1034. [doi:10.1016/j.fuproc.2007.06.010]
- Wang, Z.H., Zhou, J.H., Wen, Z.C., Cen, K.F., 2007. Effect of mineral matter on NO reduction in coal reburning process. *Energy and Fuels*, **21**(4):2038-2043. [doi:10.1021/ef0604902]
- Yang, J., Mestl, G., Herein, D., 2000. Reaction of NO with carbonaceous materials I: 1. Reaction and adsorption of NO on ashless carbon black. *Carbon*, **38**(5):715-727. [doi:10.1016/S0008-6223(99)00150-5]
- Zhao, Z.B., Li, W., Li, B.Q., 2002a. Catalytic reduction of NO by coal chars loaded with Ca and Fe in various atmospheres. *Fuel*, **81**(11-12):1559-1564. [doi:10.1016/S0016-2361(02)00077-7]
- Zhao, Z.B., Li, W., Qiu, J.S., Li, B.Q., 2002b. Catalytic effect of Na-Fe on NO-char reaction and NO emission during coal char combustion. *Fuel*, **81**(18):2343-2348. [doi:10.1016/S0016-2361(02)00174-6]
- Zhao, Z.B., Qiu, J.S., Wen L., Li, B.Q., 2003. Influence of mineral matter in coal on decomposition of NO over chars and emissions of NO during char combustion. *Fuel*, **82**(8):949-957. [doi:10.1016/S0016-2361(02)00394-0]
- Zhong, B.J., Tang, H., 2007. Catalytic effect NO reduction at high temperature by de-ashed chars with catalysts. *Combustion and Flame*, **149**(1-2):234-243. [doi:10.1016/j.combustflame.2006.04.004]
- Zhong, B.J., Zhang, H.S., Fu, W.B., 2003. Catalytic effect of KOH on the reaction NO with char. *Combustion and Flame*, **132**(3):364-373. [doi:10.1016/S0010-2180(02)00480-7]
- Zhou, H., Qiu, K.Z., Wang, Z.H., Cen, K.F., 2004. Study of coal rank and fineness on NO_x reduction with coal reburning technology. *Journal of Fuel Chemistry and Technology*, **32**(2):147-150 (in Chinese).